Geophysical Journal International

Geophys. J. Int. (2011) **185,** 1103–1119 doi: 10.1111/j.1365-246X.2011.05004.x

Crustal and uppermost mantle structure beneath the External Dinarides, Croatia, determined from teleseismic receiver functions

Josip Stipčević,[1] Hrvoje Tkalčić,[2] Marijan Herak,[1] Snježana Markušić[1] and Davorka Herak[1]

[1] *Department of Geophysics, Faculty of Science and Mathematics, University of Zagreb, Horvatovac* 95, 10 000 *Zagreb, Croatia. E-mail: jstipcevic@gfz.hr*
[2] *Research School of Earth Sciences, The Australian National University, Mills Road, Building* 61, *Canberra, ACT* 0200, *Australia*

Accepted 2011 February 25. Received 2010 December 9; in original form 2010 April 20

SUMMARY

Broad-band seismograms of teleseismic events recorded at the Croatian Seismological Network were used to compute radial receiver functions (RFs) for eight locations in the External Dinarides. Waveform modelling was performed by a multistep matching of the theoretical RFs computed for horizontally layered 1-D isotropic models with the averaged observed RFs. Constraints from existing deep seismic sounding profiles, traveltime curves of regional crustal seismic phases and intuitive inferences gained from interactive forward modelling were used to construct initial 1-D models of the Earth. A non-linear inversion was performed in two steps—a grid search followed by the Monte Carlo search for the model parameters. Concurrently, RFs from different azimuths were stacked to obtain trade-off estimates of crustal thickness versus V_p/V_s ratios. The Moho depths were found in the range from around 40 km for Northern Adriatic stations to over 55 km for stations in the central part of the External Dinarides. Comparing our results with recent maps of the Moho topography inferred from seismic and gravimetric data, we find that for some stations the agreement between our results and the existing Moho maps is very good. For the others, we find the Mohorovičić discontinuity to be considerably deeper, indicating some of the thickest crust in Europe. Although it is plausible that such a deep Moho could be a consequence of a complex tectonic setting of the region (e.g. overlapping of two large tectonic units—the Adriatic microplate and the Dinarides), this result will have to be verified in the future studies using various other geophysical techniques.

Key words: Body waves; Continental tectonics: compressional; Crustal structure; Europe.

1 INTRODUCTION

1.1 Tectonic setting

The territory encompassed by this study is located at the central part of a convergent boundary zone between the African and Eurasian plates, where their collision resulted in the formation of the Alpine–Carpathian–Dinaric mountain belt and the opening of the Pannonian basin (Fig. 1). The tectonics of the study area is shaped by the thrusting of the Adriatic microplate (Adria) into the European lithosphere. Adria is often assumed to be a promontory of Africa that broke off in Cretaceous or Tertiary (e.g. Márton 2006) and, until recently, it was assumed to be a single rigid block rotating counter-clockwise around the pole in northern Italy at an angular rate of about 0.52° Ma^{-1} (e.g. Anderson & Jackson 1987; Calais *et al.* 2002). According to new insights based on seismic data and Global Positioning System velocities, Adria is now mostly seen as two or even three smaller units (Oldow *et al.* 2002; Herak *et al.* 2005; Ivančić *et al*. 2006). The collision between Adria and Eurasia is complex and many different mechanisms to explain it have been proposed (Doglioni & Carminati 2002; Lippitsch *et al.* 2003; Brückl *et al.* 2010). The most recent geodynamic schemes suggest Eurasia subducting under the Adria in the whole Alpine region, together with a less pronounced underthrusting of the Adria beneath the Eurasia at the northeastern collisional boundary (Doglioni & Carminati 2002; Brückl *et al.* 2010). Along the northeastern coast of the Adriatic Sea this process resulted in the formation of the Dinarides and thickening of the crust. Current deformation rate on the Adria–Dinarides contact amounts to about 3–4 mm yr^{-1} (e.g. Nocquet & Calais 2004; Brückl *et al.* 2010). The Dinarides are the thrust and fold belt zone of elevated and highly folded sediments that stretches along the northwest–southeast direction, from the Southern Alps in the north to the Albanides in the southeast. To the northeast Dinarides are bounded by the Pannonian basin with a wide transition zone in between (Šumanovac *et al.* 2009; Brückl *et al.* 2010). Many recent studies have investigated the NW Dinarides (Brückl *et al.* 2007; Šumanovac *et al.* 2009; Brückl *et al.* 2010), primarily focusing on the 'triple junction' between Adria, the European plate (Alps) and

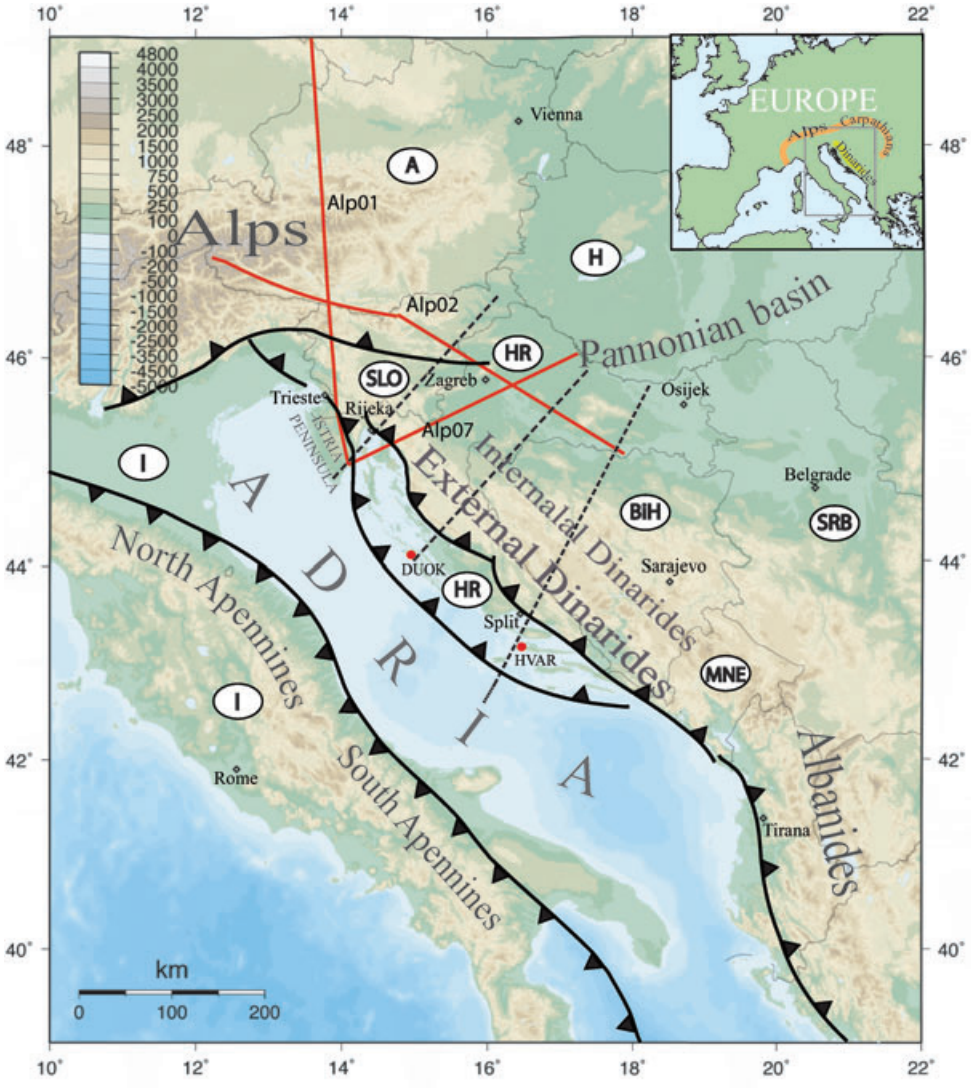

Figure 1. Map of the regional tectonic setting in the wider regional context (see inset). Black lines with barbs indicate main faults in the region (generalized after Tomljenović 2002 and Faccenna *et al*. 2004). DSS profiles shown with dashed black lines are from the experiments conducted in 1960s, while the Alp2002 DSS profiles are marked by solid red lines. Two stations marked with red circles are the locations for which receiver functions analysis has been previously done (van der Meijde *et al.* 2003). A, Austria; BiH, Bosnia and Herzegovina; H, Hungary; HR, Croatia; I, Italy; MNE, Montenegro; SLO, Slovenia; SRB, Serbia.

the Pannonian fragment, which they locate near the Tauern window in southern Austria. Other parts of the Dinarides are not so well investigated but recent work suggests at least local underthrusting of Adria beneath External Dinarides in their Central part (Šumanovac 2010a) and still active subduction in most of the southern part (Piromallo & Morelli 2003; Bennett *et al.* 2008).

1.2 Previous work and motivation

The earliest investigation of the lithosphere beneath Croatia using seismic waves was conducted by Mohorovičić following the Kupa valley earthquake of 1909 (Mohorovičić 1910). In his paper Mohorovičić described two distinct pairs of *P* and *S* phases, for one of which he correctly assumed to have been generated at the structural discontinuity beneath the surface of the Earth. Based on the recordings of this and other earlier earthquakes at about two dozen seismographs operating in Europe at that time, he calculated that the discontinuity is located at the depth of about 54 km. Since then many seismic studies have been conducted regarding the lithospheric structure beneath Croatia. These include deep seismic sounding (DSS) experiments (Dragašević & Andrić 1968; Aljinović 1977; Aljinović 1983; Aljinović *et al*. 1984; Brückl *et al.* 2007; Šumanovac *et al.* 2009), body-wave traveltime analysis (Herak 1990; Herak & Herak 1995) and the analysis of *P* to *S* waves converted at the Moho for a wider region including two stations located in Croatia (van der Meijde *et al.* 2003).

First DSS experiments in Croatia were performed in 1960s by the state-owned company (Geofizika) on three profiles stretching from the Adriatic coast to the continent with the general southwest–northeast direction (Fig. 1). Results from these experiments (Aljinović 1983; Skoko *et al.* 1987) suggest crustal thickness ranging between 20 and 45 km, with the thickest crust beneath the Dinarides, and the crust thinning rapidly towards the Pannonian basin in the northeast and the Adriatic in the southwest. The experiments also mapped a crustal discontinuity at the transition zone between a carbonate-rich sedimentary cover and the

crystalline basement with an average depth of 10 km. Another set of three DSS experiments (Alp01, Alp02 and Alp07) was recently performed as part of the larger ALP 2002 experiment investigating lithospheric structure of the Eastern Alps and the surrounding areas. The Alp01 and Alp02 profiles (Brückl *et al.* 2007) only partially transected Croatia (Fig. 1), their southern parts covering the Istria peninsula and the SW Pannonian Basin, respectively. The Alp07 profile (Šumanovac *et al.* 2009) was laid out entirely in Croatia with the SW–NE trend and the endpoints in the Istria peninsula and the SW Pannonian basin (Fig. 1). Their interpretation points to a two-layered crust beneath the NW Dinarides, with low seismic velocities (5.8–6.1 km s^{-1}) in the upper crust and relatively high *P*-wave velocities (6.4–7.1 km s^{-1}) in the lower crust. The Pannonian crust is found to be well represented by a one-layered model with seismic velocities of 5.7–6.1 km s^{-1}, and with a relatively broad transition zone at the border with the Dinarides. Their experiments also confirmed a general scheme of the thickest crust under the Dinarides with the thickness decreasing from 40 km in the NW Dinarides to 25 km in the Pannonian basin and 30 km in the Adriatic. Analysis of seismic body-wave velocities in the circum Adriatic region by Herak & Herak (1995) showed similar results. They found velocities of 5.8–6.1 km s^{-1} and about 6.4 km s^{-1} in the upper and topmost lower crust, respectively. The sub-Moho velocities ranged from over 8.0–8.2 km s^{-1} in the Pannonian basin and the Alps, to 7.8–8.1 in the Dinarides. The average crustal thickness of 40 km in the Dinarides was indicated to generally increase towards the southeast and reach over 55 km in their southernmost part.

With the accumulation of crustal structure data, many detailed maps of Moho for Europe have been compiled in the recent years (e.g. Ziegler & Dèzes 2006; Tesauro *et al*. 2008; Grad *et al*. 2009). Primary data source for most of these maps have been the DSS experiments, whereas in the areas with no DSS coverage data from other geophysical investigations were used. For the Dinarides and the surrounding areas all such compilations suffer from lack of measurements, which results in high uncertainties in estimations of the Moho depths. Crustal structure of the Pannonian basin is reasonably well known due to the petroleum and gas exploration (Saftić *et al.* 2003), but the amount of data for other parts of Croatia and the neighbouring Bosnia and Herzegovina is limited. Although the general scheme of plate dynamics is not disputable, regions of great interest such as the central and the southern part of the Dinarides are poorly sampled, and details of the underlying tectonic structures remain largely unexplained.

In the past few decades teleseismic receiver function (RF) method has become one of the most reliable and commonly used techniques to determine crustal structure under the three-component broad-band seismographs (e.g. Langston 1979; Owens *et al.* 1987; Ammon 1991; Sandvol *et al.* 1998; Park & Levin 2000; Julia *et al.* 2003). This widely applied method presents an elegant and effective way of isolating the Earth's response beneath the recording station by deconvolving the vertical *P*-wave component from its radial component.

RF studies in Croatia have, until now, been limited to only two locations in the Adriatic islands (van der Meijde *et al.* 2003). They reported a two-layered crust and the Moho depths of 41 km and 47 km beneath the stations DUOK (island of Dugi Otok) and HVAR (island of Hvar), respectively (Fig. 1). Lithosphere beneath stations located on the western coast of the Adriatic was investigated using RFs by, for example, Piana-Agostinetti *et al*. (2002), Mele & Sandvol (2003), Di Bona *et al.* (2008) and Piana-Agostinetti & Amato (2009). The results for western Adriatic stations indicate crustal thickness ranging from 30 to 35 km and the crust thinning

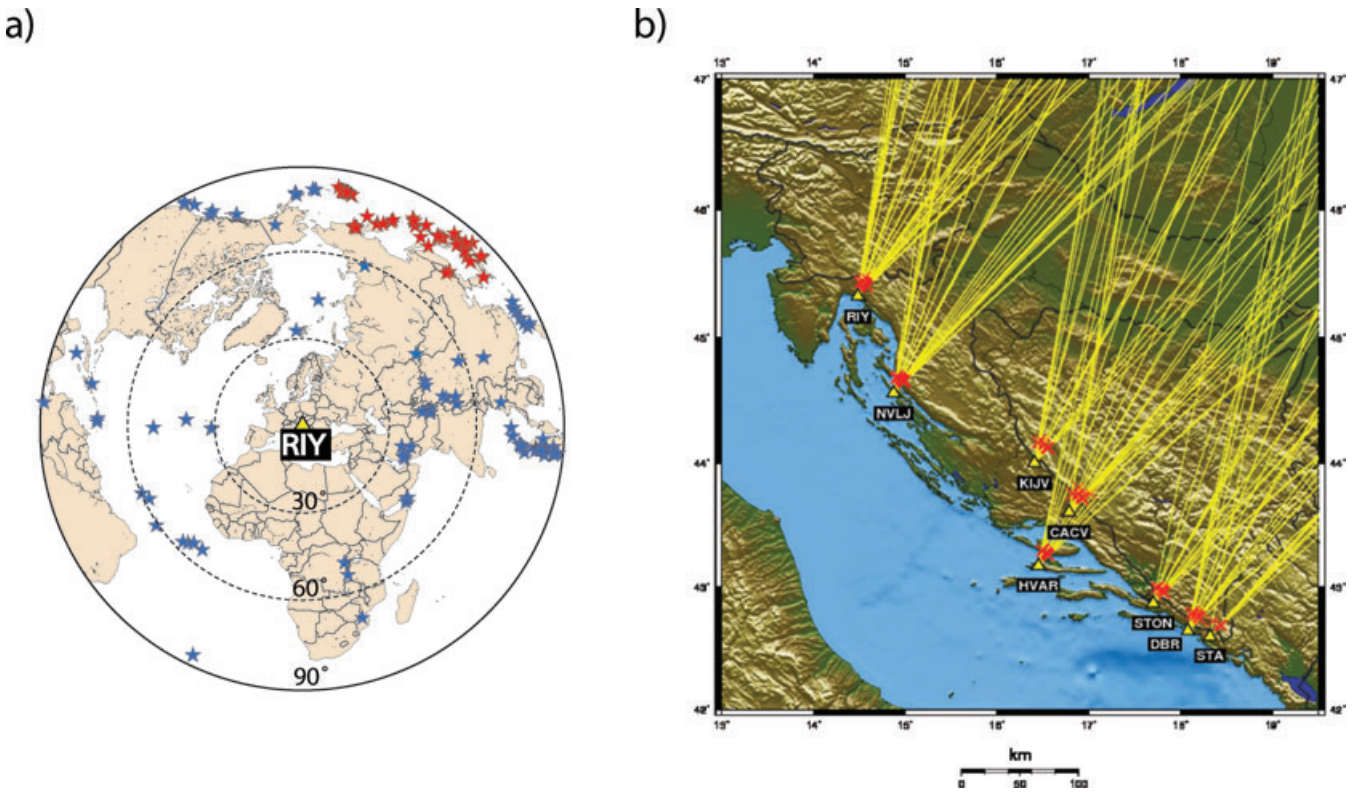

Figure 2. (a) Global distribution of the events recorded at the station RIY (Rijeka) used here (M_w > 5.5 from 2002 January to 2008 July). Red stars mark earthquakes selected for this study. (b) Distribution of the eight stations (triangles) with ray paths used to obtain representative receiver functions for particular stations. Red crosses denote the vertical surface projection of the Moho piercing point of each ray.

towards the east. Similarly, RFs were recently used to study the lithospheric and upper-mantle structure beneath the central and eastern Europe (Geissler *et al.* 2008). Their results obtained for two stations located along the Adriatic coast indicate thick crust. For the northern Adriatic station (Trieste, Italy), crustal thickness of 39 km is reported, while their results for the southern Adriatic station (Tirana, Albania) suggest Moho at the depth of 54 km.

Depths to the Mohorovičić discontinuity and details of crustal structure of the Dinarides are crucial for understanding the geodynamic processes there. With the main goal to improve constraints on the Moho depth and to investigate the crust for other major discontinuities, we here analyse teleseismic RFs corresponding to the broad-band waveforms recorded by the Croatian Seismic Network (CSN) at all stations continuously operating for more than 18 months. The results of analyses using multiple techniques of inverse and forward modelling are used to construct the new regional map of the Mohorovičić discontinuity of the coastal part of Croatia, taking into account eight new data points.

2 DATA

During the last decade, the Department of Geophysics of the Faculty of Science of the University of Zagreb has invested significant efforts to build and maintain modern digital seismological network. The main goal of this network is to monitor and report seismic activity in Croatia and the surrounding areas. In this process, a large amount of high-quality waveform data suitable for various seismic studies has been collected. The data utilized in this study consists of teleseismic recordings from eight available permanent broad-band stations of CSN. Operation duration for specific sites range from 18 months to 10 yr. All of the stations used are located on or very near the coast of the Adriatic Sea, close to the boundary of Adria and the External Dinarides (Fig. 2).

Data used to estimate RFs consist of three-component broad-band seismograms for earthquakes with magnitudes $m_b > 5.5$ and epicentral distances between 30° and 90°. The number and waveform quality of recorded events for a specific station depend on the station operation length, occasional instrumental malfunction, ambient noise and site conditions. As an example, global distribution of recorded events for the Northern Adriatic station RIY (Rijeka) is presented in Fig. 2(a). For the majority of stations, the number of recorded events varied between 110 and 170, except for the stations STA (Stravča) and CACV (Čačvina) that recorded 89 and 48 events, respectively. After removing noisy signals, the number of the events that produced stable RFs ranged between 42 and 108 (Fig. 3b and Table 1).

3 METHOD

The data are analysed by a combination of the grid-search, forward modelling and the Monte Carlo search. Prior to applying various forward and inversion techniques to model *S*-wave velocity structure beneath each station, *a priori* information was collected from existing DSS profiles and regional traveltime curves. A combination of grid-search and interactive RF forward modelling were used to construct starting and intermediate models. During the interactive modelling the misfit between the observed and the theoretical RFs is minimized by manually adjusting velocities and thicknesses of individual layers. This intermediate model is then refined by a Monte Carlo search of model parameters. To reduce ambiguity in identifying crustal thickness, we also perform the H-κ domain (thickness – V_p/V_s ratio) search assuming a single-layered crust with average crustal properties (Zhu & Kanamori 2000). In the following, we describe each step in more detail.

3.1 Processing of RFs

RF analysis relies on the fact that impinging teleseismic *P* waves convert to *S* waves at the sharp impedance contrasts. For the steeply

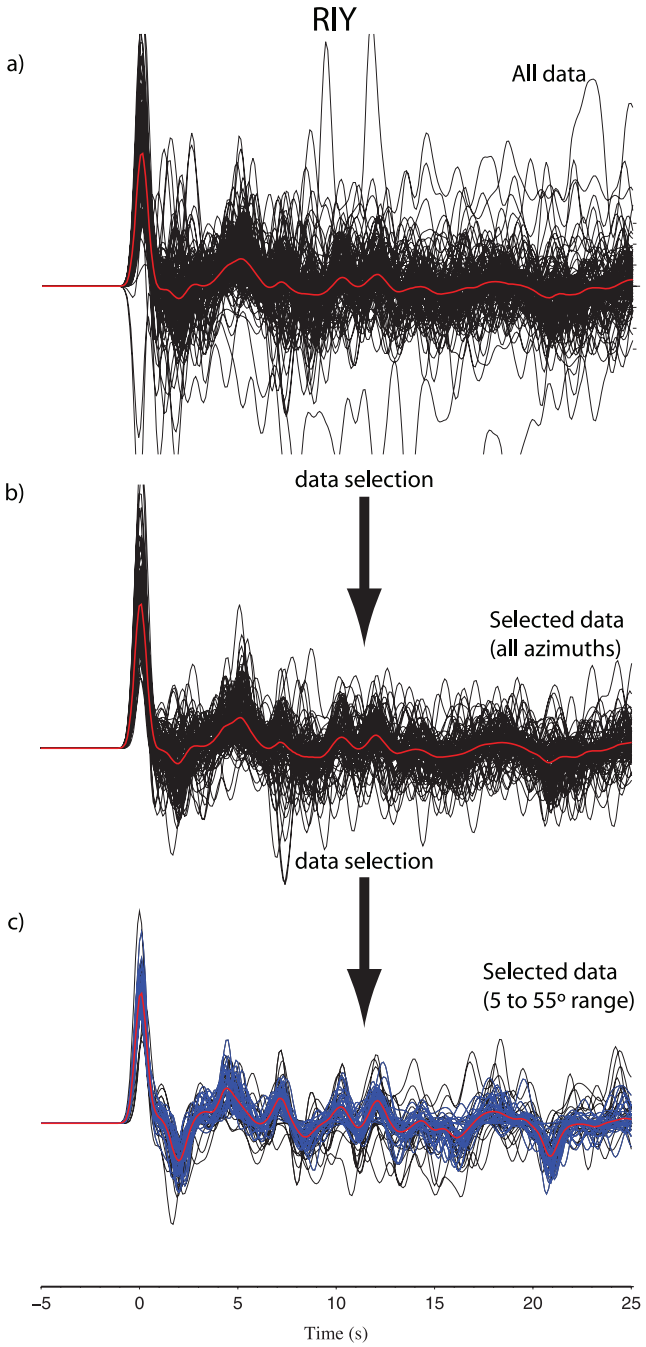

Figure 3. Example of receiver function selection process for the station RIY located in the Northern Adriatic. Average receiver faction for each data selection is shown in red. (a) Radial receiver functions for low-pass Gaussian filter width parameter 2.5 from data corresponding to all available events shown in Fig. 2(a) (from all backazimuths). (b) RFs left after eliminating outliers and noisy records. (c) RFs left after selecting only events from the northeastern backazimuths (black) and after performing a selection based on the coherency of the waveforms (blue).

Table 1. The Moho depth resulting from the Monte Carlo waveform inversion and the H-κ search method (for $V_p = 6.4$ km s^{-1}), along with the values of V_p/V_s and locations of all stations included in this study. For the stations CACV and HVAR the values related to the two most prominent maxima in H-κ search are given. The number in parentheses in columns giving the Moho depth shows the numbers of RF used. Uncertainties for the H-κ results indicate the total range of bootstrap solutions for all three average *P*-wave velocities ($V_p = 6.2$, 6.4 and 6.6 km s^{-1}).

Station code	Latitude (°N)	Longitude (°E)	Moho (km) inversion	Moho (km) H-κ	Moho mean value (km)	V_p/V_s H-κ
RIY	45.3251	14.4828	$39 \pm 2(33)$	$42.6 \pm 0.8(107)$	40.8	1.71 ± 0.02
NVLJ	44.5635	14.8711	$43 \pm 2(27)$	$36.9 \pm 0.4(64)$	40.0	1.92 ± 0.01
KIJV	44.0500	16.4047	$60 \pm 2(15)$	$50.6 \pm 14.6(80)$	55.3	1.89 ± 0.14
CACV	43.6089	16.7844	$56 \pm 2(15)$	57.5 ± 7.8 or $44.6 \pm 7.8(42)$	52.7	1.72 ± 0.09 or 1.94 ± 0.09
HVAR	43.1776	16.4490	$46 \pm 1(17)$	37.9 ± 7.7 or $46.1 \pm 7.7(97)$	43.3	1.92 ± 0.12 or 1.76 ± 0.12
STON	42.8710	17.6999	$47 \pm 2(14)$	$40.4 \pm 5.6(64)$	43.7	1.89 ± 0.16
DBR	42.6473	18.0787	$55 \pm 2(20)$	$44.4 \pm 1.9(103)$	49.7	1.90 ± 0.03
STA	42.6008	18.3183	$48 \pm 3(8)$	$42.5 \pm 1.8(72)$	45.2	1.89 ± 0.04

incident *P* waves, *P*-to-*S* converted waves are mainly recorded on the horizontal components. To isolate effects of local structures recorded on horizontal components these components are deconvolved with the vertical component (Langston 1979; Ammon 1991). The resulting waveform is termed the 'receiver function' and represents the transfer function of the medium beneath the recording station.

Radial RFs are computed using the time-domain iterative deconvolution procedure described by Ligorría & Ammon (1999). Compared to the 'water-level' deconvolution procedure in the frequency domain this method requires more computational time but produces more stable results for the low signal-to-noise ratio data. Prior to computing RFs a visual inspection of the earthquake records is performed to exclude waveforms without a clear *P*-wave arrival. Also, to remove higher frequency noise but still keep high enough resolution to detect smaller subsurface structures, a low-pass Gaussian filter with a width-parameter $a = 2.5$ is applied, which in the time-domain corresponds to the width of the Gaussian pulse of 2.64 s. One such group of RFs is shown in Fig. 3(a). After the RFs were computed, another visual examination of the data was carried out to eliminate outliers and noisy records.

From such a consolidated data set (Fig. 3b), only data from backazimuths in the range 5°–55° and with distances larger than 75° (which roughly corresponds to ray parameters in the range 0.055–0.040 s km^{-1}) were retained (Fig. 3c). This was done to ensure that all data for all stations correspond to similar, in this case mostly continental, ray paths. This particular range of backazimuths and distances, corresponding mostly to earthquakes from the Aleutian Islands and the Japan region, was chosen after some trial-and-error as it provided enough data on all stations. By choosing only one azimuthal range with a narrow interval of ray parameters, we have consciously set the issues in conjunction with a possible Moho dip and anisotropy aside. Although the question of azimuthal variation of RFs will have to be addressed in future studies, based on comparison of amplitudes of radial and transversal components of RFs on all stations, we estimate that it is not significant in the context

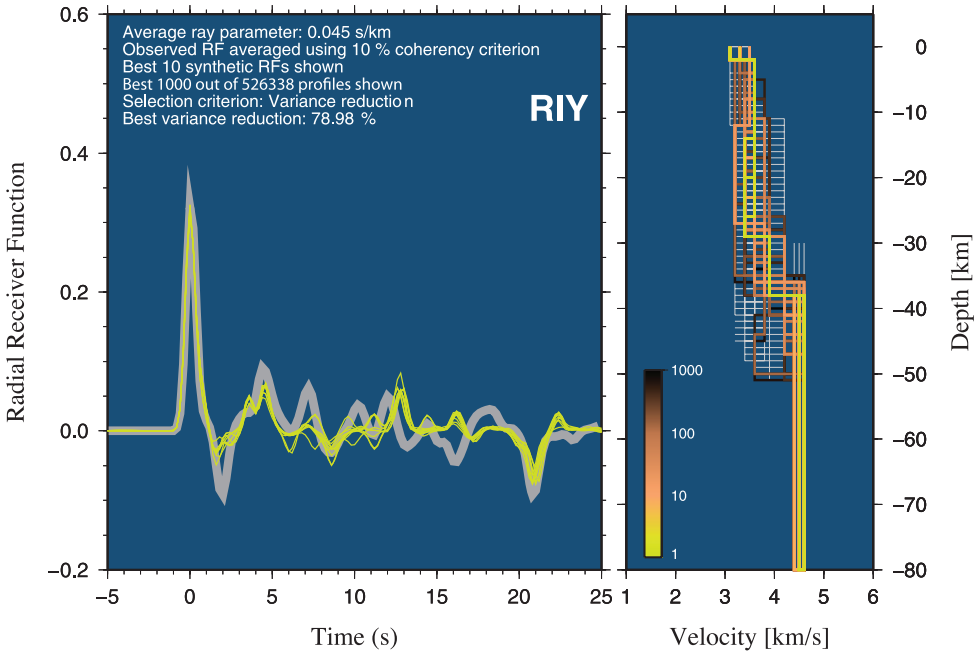

Figure 4. Grid search results (with three layers in the crust and a half-space in the mantle) for lithospheric structure after modelling RFs (low-pass Gaussian filter width parameter 2.5) for the station RIY. Thick grey line on the left-hand side is the averaged observed receiver function (marked red in Fig. 3c) and the thin yellow lines are theoretical RFs for 10 best shear wave velocity profiles shown on the right-hand side. Velocity profiles for 1000 best models obtained in the grid search are shown on the right hand side. The range of the grid search is shown by thin grey lines and is selected based on constraints from previous studies.

of meeting our goal of constructing the first-order approximations for 1-D models of the crust and uppermost mantle.

To select only the most coherent waveforms from the chosen backazimuth range, an additional statistical test was performed as in Tkalčić *et al.* (2006). From a matrix of cross-correlation coefficients for each pair of RFs, only those RFs are extracted that cross-correlated well (with the cross-correlation coefficient of 0.9 and higher) with at least 5 per cent or 10 per cent of other RFs. This percentage is estimated empirically by visually examining the coherency of the extracted waveforms (blue lines in Fig. 3c). The representative RF at each station is then constructed by averaging the RFs extracted as described above (red line in Fig. 3c).

3.2 Multistep forward and non-linear inverse modelling

Because there is little *a priori* information about structures under the stations used, a grid-search method is employed to place more constraints on the simple starting model. Grid-search is

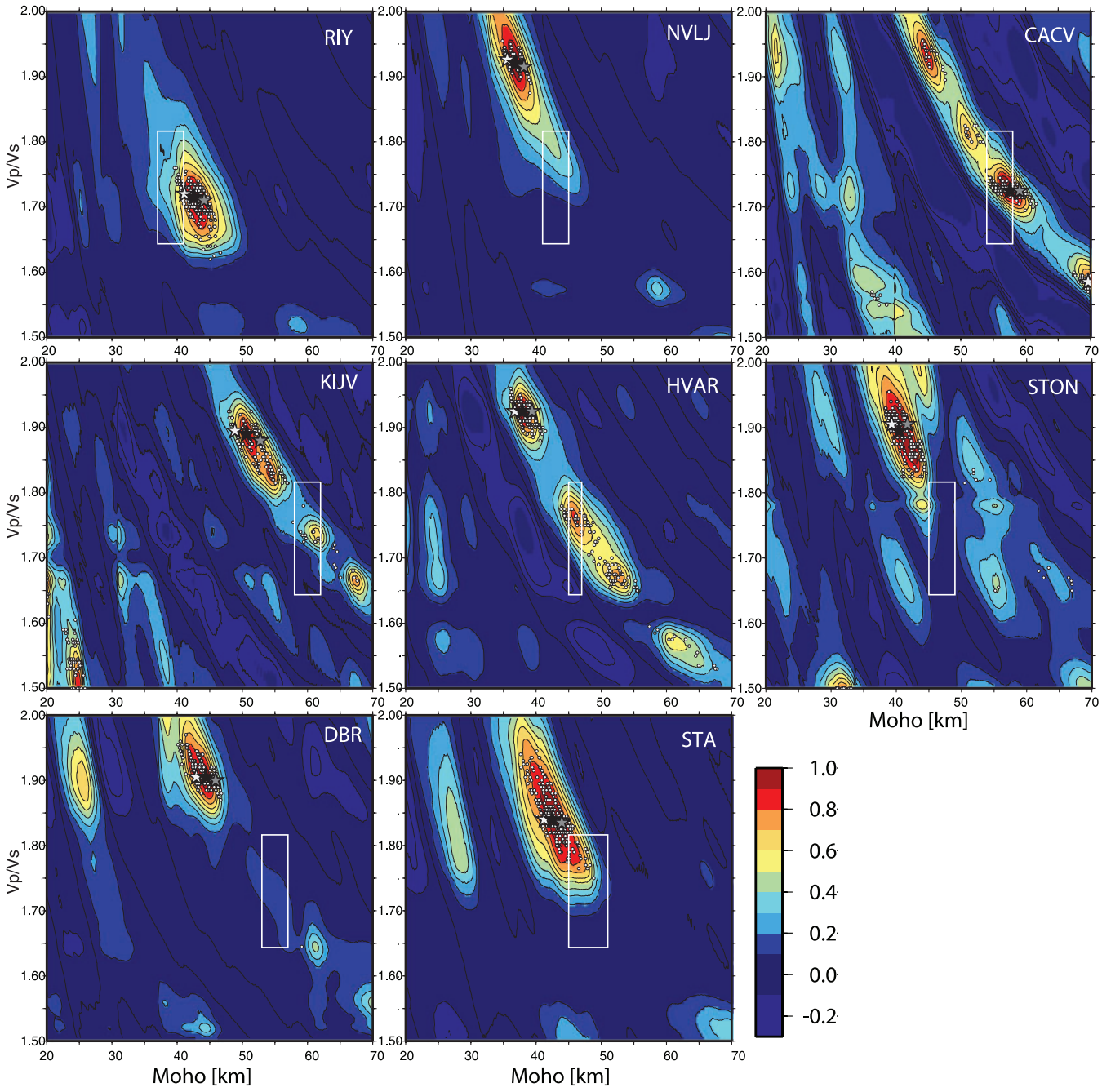

Figure 5. Results of the modified H-κ domain search method (Niu & James 2002; Chen *et al.* 2010) for the stations RIY, NVLJ, KIJV, CACV, HVAR, STON, DBR and STA using the average crustal V_p value equal to 6.4 km s^{-1}. The black star denotes the position of the optimal solution for the crustal thickness and the V_p/V_s ratio. Light and dark grey stars indicate best solutions corresponding to V_p values of 6.2 and 6.6 km s^{-1}, respectively. Light grey dots are the results from bootstrap resampling algorithm. The area bounded by the solid line box indicates range of values from the inversion using the Monte Carlo search (see Fig. 6).

advantageous because it searches through the whole pre-defined parameter space and minimizes possible bias due to a poor starting model (Fig. 4). Although this approach is computationally intensive and more time-consuming it results in more accurate modelling. The grid-search was performed following the approach of Tkalčić *et al.* (2006). The parameter space used consisted of three layers over a half-space, assuming the Poisson ratio of $\sigma = 0.25$ and the Birch law (Birch 1961) for density, with the grid spacing of 1 km for layer thickness and 0.3 km s^{-1} for the shear wave velocity. Among obvious disadvantages of this method is the fact that the resulting models are often too simplistic and fail to model less significant structures in the crust.

To address the shortcomings of the grid-search mentioned, we subsequently run a Monte Carlo search. The reference model for the search is defined by subdividing the best model found by the grid-search into layers 5–7 km thick, depending on the Moho depth in the model. The topmost one or two layers—set to be between 0.5 and 4 km thick—are introduced to account for the sedimentary layers close to the surface. $V_p/V_s = 1.73$ is kept constant for all layers. For the layers located in the uppermost mantle, the thickness

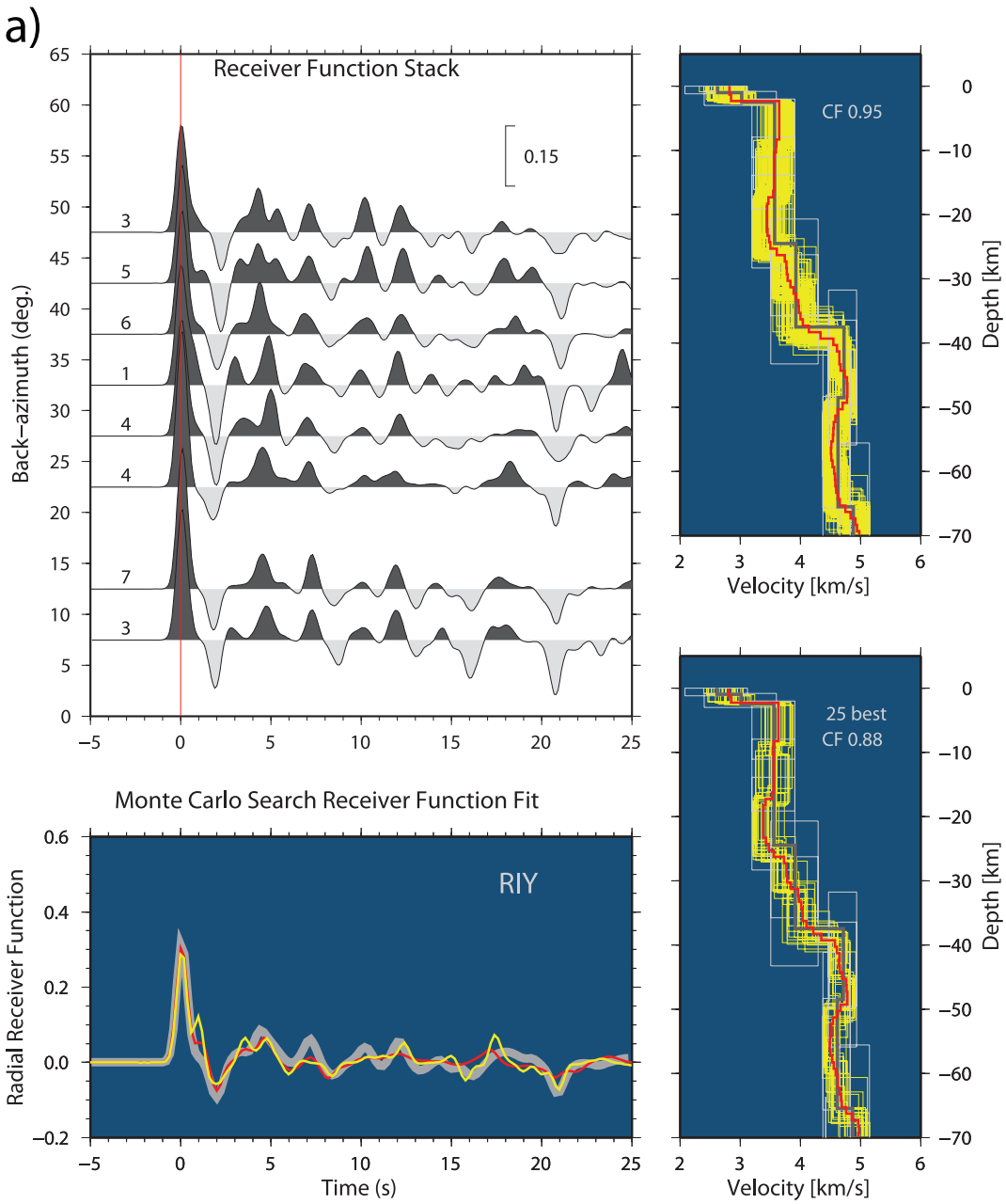

Figure 6. Monte Carlo search results for structure beneath eight Croatian stations after fitting the observed receiver function (thick grey line in the lower left-hand side). The upper left subplot displays observed RFs stacked in azimuthal bins of 5° for the backazimuth range of 5–55°. The numbers above each trace give the number of averaged RFs in each azimuth bin. In the upper and lower subplots on the right, thick grey lines show the starting model from the grid search and interactive modelling (IRFFM); the thin white lines represent the bounding boxes for parameter variation (shear wave velocity and thickness) in each layer of the starting model. Thin yellow lines are the resulting models inside the 95 per cent confidence interval (upper right), and the 25 best fitting models (lower right-hand side). Thick red lines show the averaged model. In the lower left, the RF calculated from the single best-fitting model is displayed in yellow, and the RF from the averaged model is shown in red. Stations are presented in the order from northwest to southeast.

of 10–15 km is assumed. This model is then further improved by interactively adjusting the thicknesses and layer velocities by the IRFFM (Interactive Receiver Functions Forward Modeller) computer program (Tkalčić & Banerjee 2009) until the maximum variance reduction is obtained, and a good fit is achieved between the observed and the theoretical RFs. Attention was paid to reproduce as closely as possible the onset times, as well as the amplitudes of the most prominent peaks. Although some degree of subjectivity is thus introduced, it is our experience that the process quickly leads to a plausible and realistic intermediate model, which is not always the case with automatic inversions. Furthermore, the synthetic tests we performed show that, after some experience is gained, fairly complex crustal models can be reasonably well reconstructed by this approach.

With a starting model created as described, a Monte Carlo search is performed—100 000 models are generated by randomly varying layer parameters within the pre-defined bounds, which amount to ±15–20 per cent for the thicknesses, ±5–20 per cent for the shear wave velocities and 5 per cent for the V_p/V_s ratio. Small variation of 5 per cent in velocities and 15 per cent in layer thickness has been introduced in the starting model for layers beneath the Mohorovičić discontinuity where we expect smaller overall variation in both parameters. For layers in the crust we set 10 per cent variation for *S*-wave velocity and 15 per cent variation for layer thickness. In the two layers closest to the surface, where expected variations as well as the uncertainties are the largest, we use the maximum variance of 20 per cent for both parameters. This step proved important in fitting our calculated RFs to the measured ones because the thin layers with

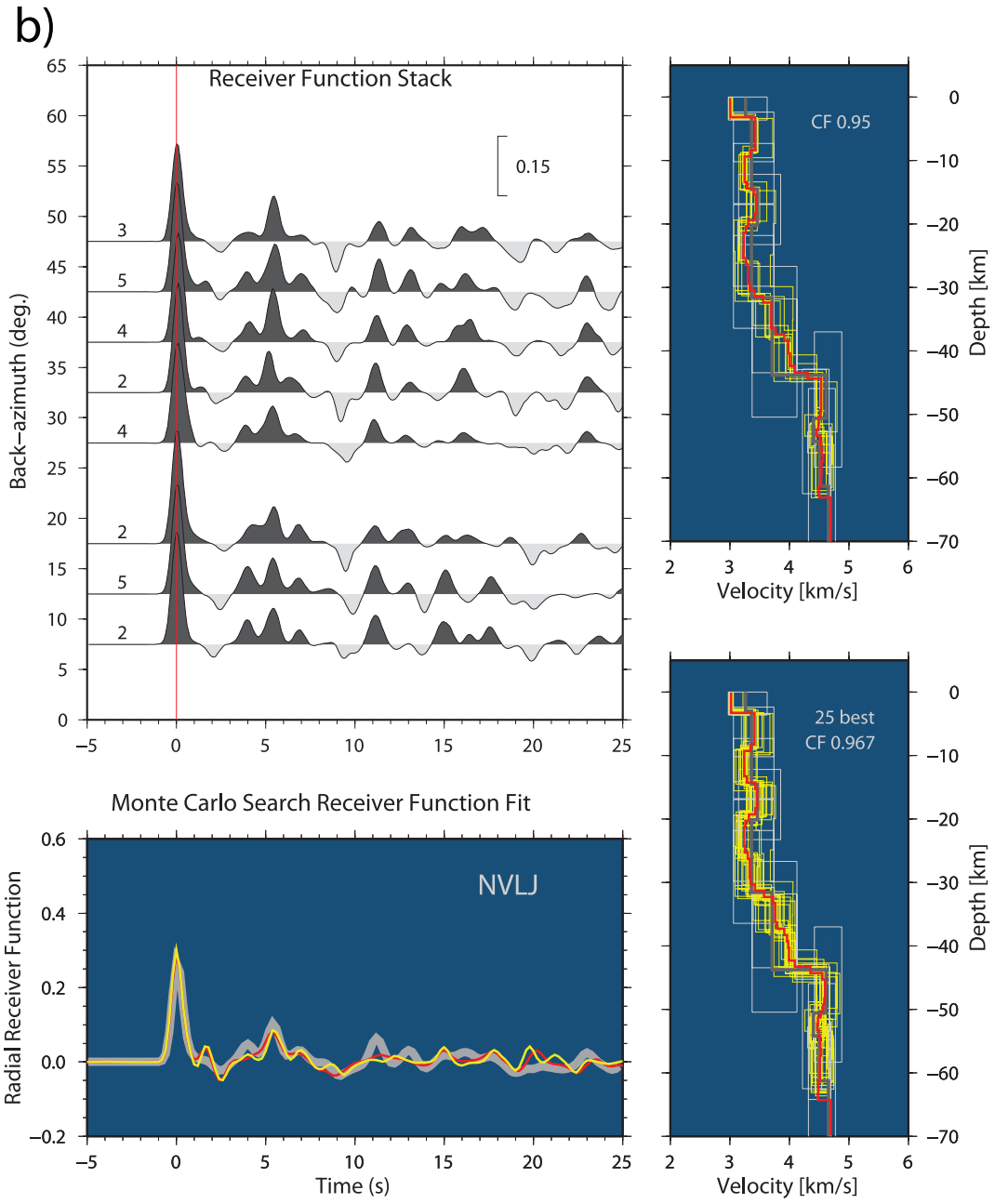

Figure 6. (*Continued.*)

very small velocities close to surface have large influence on the amplitudes of RFs (Cassidy 1992).

To construct confidence intervals, for each generated model we normalize the respective misfit function by the minimal one, $f_i = S_i/S_0$, and compute the F-function cumulative distribution $F_i = \mathrm{CDF}(f_i, N–m, N–m)$, where S_i and S_0 are the mean squared residuals for the ith model and for the best fitting model, respectively, N is the number of samples and m is the number of varied model parameters (e.g. Mayeda *et al*. 1992; Bianco *et al*. 2002). Next, all the models falling within the 95 per cent confidence interval ($F_i < 0.95$) are averaged to form a final model for each station.

3.3 H-κ stacking

The H-κ stacking technique featured in Zhu & Kanamori (2000) and Chevrot & van der Hilst (2000) calculates the predicted arrival times of the main Moho phases (P_s, P_pP_s, $P_pS_s + P_sP_s$) for each pair of H (Moho depth) and $\kappa = V_p/V_s$ values, and stacks the values of the observed RFs at those times. To emphasize the phases that are more pronounced, appropriate weights are assigned to each phase. Here we use weights of 0.5, 0.25 and 0.25 for P_s, P_pP_s and $P_pS_s + P_sP_s$ phases, respectively. The best estimates of crustal thickness and the V_p/V_s ratio are found when the main observed Moho phases result in a high amplitude stack.

Although the H-κ domain search provides a quick and effective way to estimate the crustal parameters (H and V_p/V_s) there are limitations when using this technique because of the trade-off between H and κ throughout the H-κ domain. To minimize this trade-off we have used the modified H-κ stacking technique (Niu & James 2002; Chen *et al.* 2010), which reduces the trade-off effect by calculating the coherence between the P-to-S conversions and the reverberation phases at different κ values (for further details see Chen *et al.* 2010).

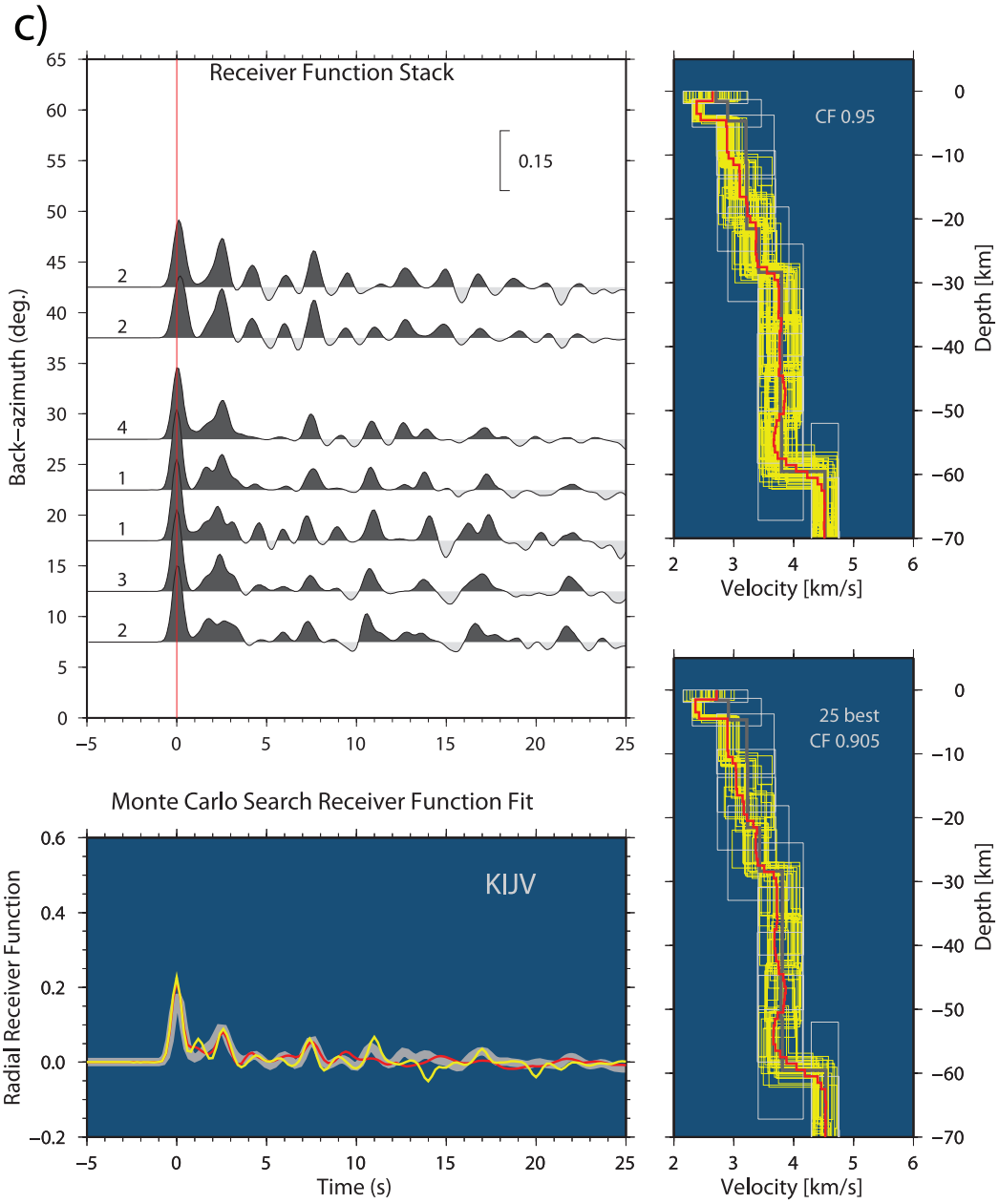

Figure 6. (*Continued.*)

In the H-κ domain search, RFs from all backazimuths are used to get information about average crustal properties and the Moho depth. Furthermore, results from H-κ method enabled us to constrain the range of the interactive forward modelling using the IRFFM software (see above) and the Monte Carlo search, which significantly reduced computational time. H-κ search was performed for three average *P*-wave velocity values within the crust, $V_p = 6.2$, 6.4 and 6.6 km s^{-1}. They were chosen after Christensen & Mooney (1995), who report $V_p = 6.4 \pm 0.25$ km s^{-1} for young orogenic areas (such as the Dinarides), and also taking into account studies of the crustal structure done by Herak & Herak (1995) and Herak (1990). Comparison of the results produced using the three V_p values provides an estimate of stability of the solutions (Piana-Agostinetti & Amato 2009), and indicates the epistemic variability caused by that input parameter. To cover the entire range of expected values in the studied area we applied the H-κ search in the range of 20–70 km for the crustal thickness and 1.5–2.0 for V_p/V_s. The contours of stacked weighted RF amplitudes of main converted phases sampled at theoretical onset times for a respective model are shown in Fig. 5 for the intermediate $V_p = 6.4$ km s^{-1}, along with alternative solutions for other two velocities. The best solutions using the bootstrap method (Efron & Tibshirani 1986) with 100 resampled sets for each of the velocities are also shown as small grey circles. In general, Fig. 5 reveals that numerically preferred solutions in many cases correspond to very high V_p/V_s ratios, even exceeding 1.9.

4 RESULTS

Figs 6(a)–(h) illustrate the results of inversions performed by the Monte Carlo search as outlined earlier for all eight stations: RIY,

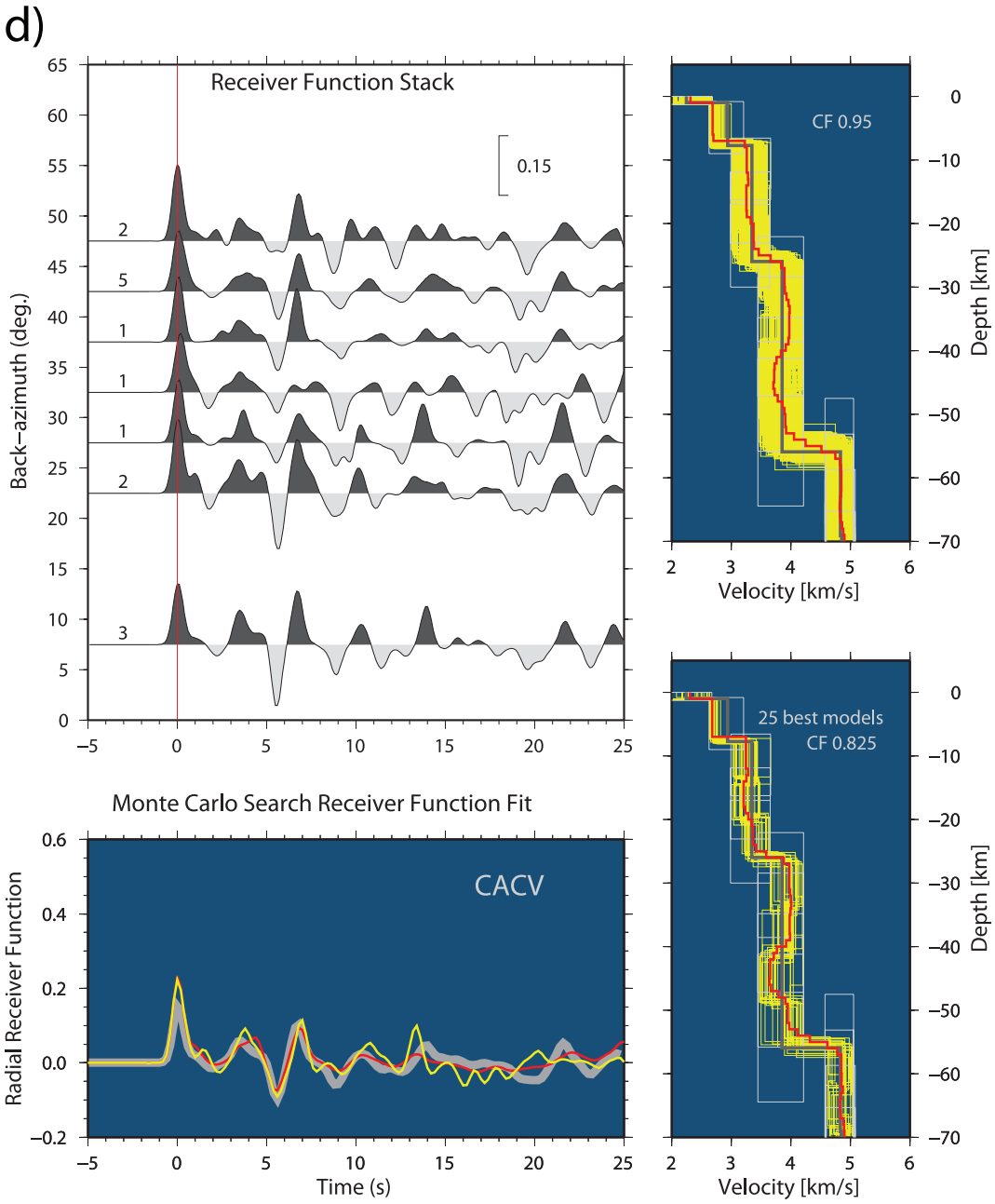

Figure 6. (*Continued.*)

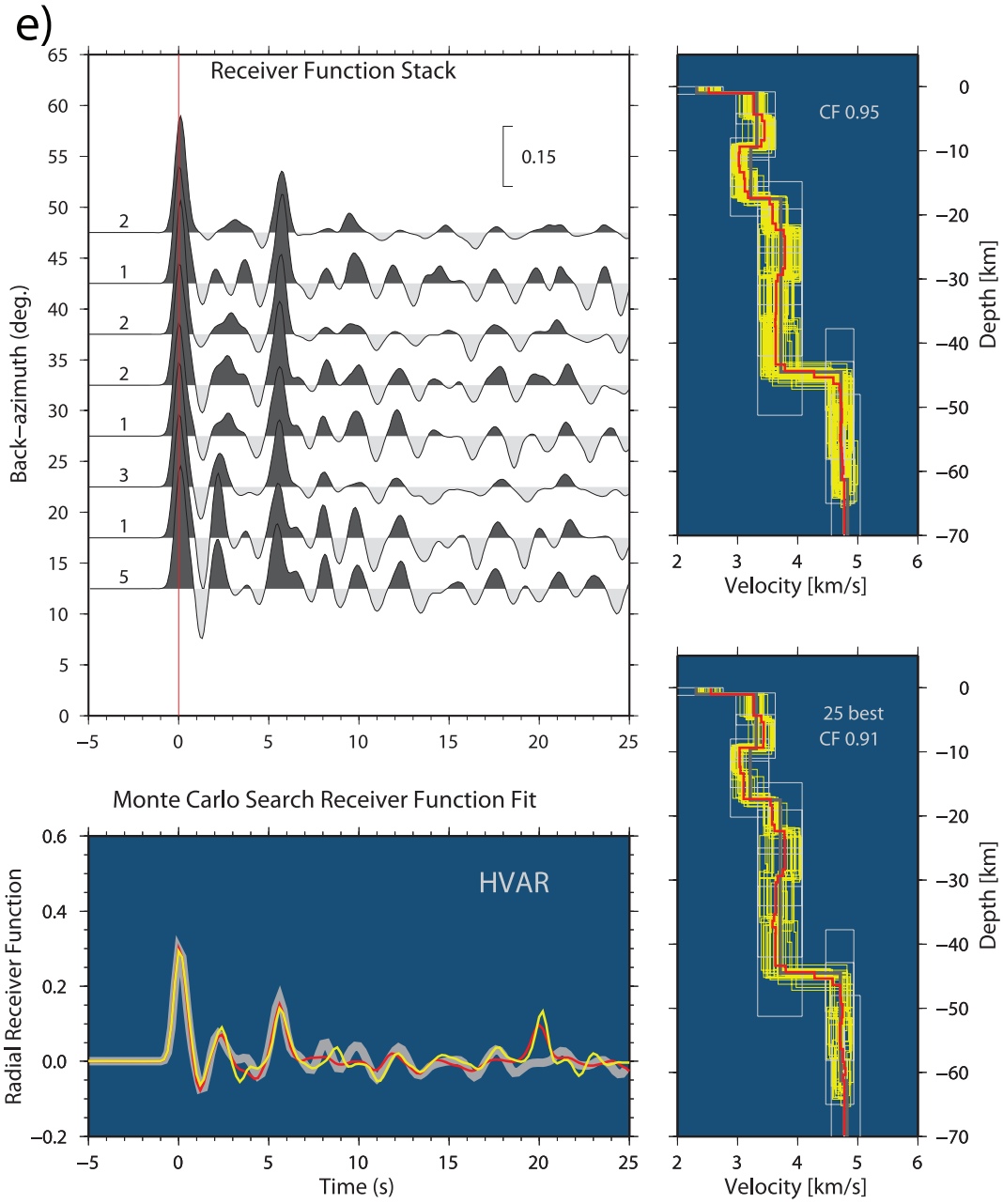

Figure 6. (*Continued.*)

NVLJ (Novalja), KIJV (Kijevo), CACV, HVAR, STON (Ston), DBR (Dubrovnik) and STA. In the following, the average model found (red line in the top-right subplot in Figs 6) will be used to describe inferred properties of the crust and uppermost mantle at each station. It should be noted that this model is only representative of the average properties of a multitude of individual models which all describe observations equally well (at the chosen confidence level). It is further used only together with appropriate measure of uncertainty (e.g. in description of modelling results and in Table 1) to describe average findings or for comparison with results of the H-κ modelling. Table 1 presents a summary of results for the Moho depth and the V_p/V_s ratio obtained by the inversion and the H-κ method.

The station RIY (Fig. 6a) is located in the Northern Adriatic at the western edge of the NW Dinarides. The crust of this area is shaped by the transition from the Dinaric crust in the east to the crust of the Adria microplate in the west. The inversion results match very well the interpretations of the Alp07 DSS profile. We found a predominantly two-layered crust with a 3-km-thick layer of low seismic velocities above the upper crust. The upper crust has relatively high and constant velocities that decrease slightly until the transition to the lower crust, which starts around the depth of 26 km. Seismic velocities in the lower crust increase relatively quickly up to the crust–mantle boundary, which appears to be gradational and with average depth of 39 $\pm$ 2 km. The results from the H-κ method (Fig. 5) indicate somewhat deeper Moho of 43 $\pm$ 1 km with a V_p/V_s ratio within the crust of 1.71 $\pm$ 0.02.

NVLJ (Fig. 6b) is another North Adriatic station, situated on the island Pag, slightly westwards of the Dinarides. The results of the inversion and the H-κ stacking indicate crustal thickness of

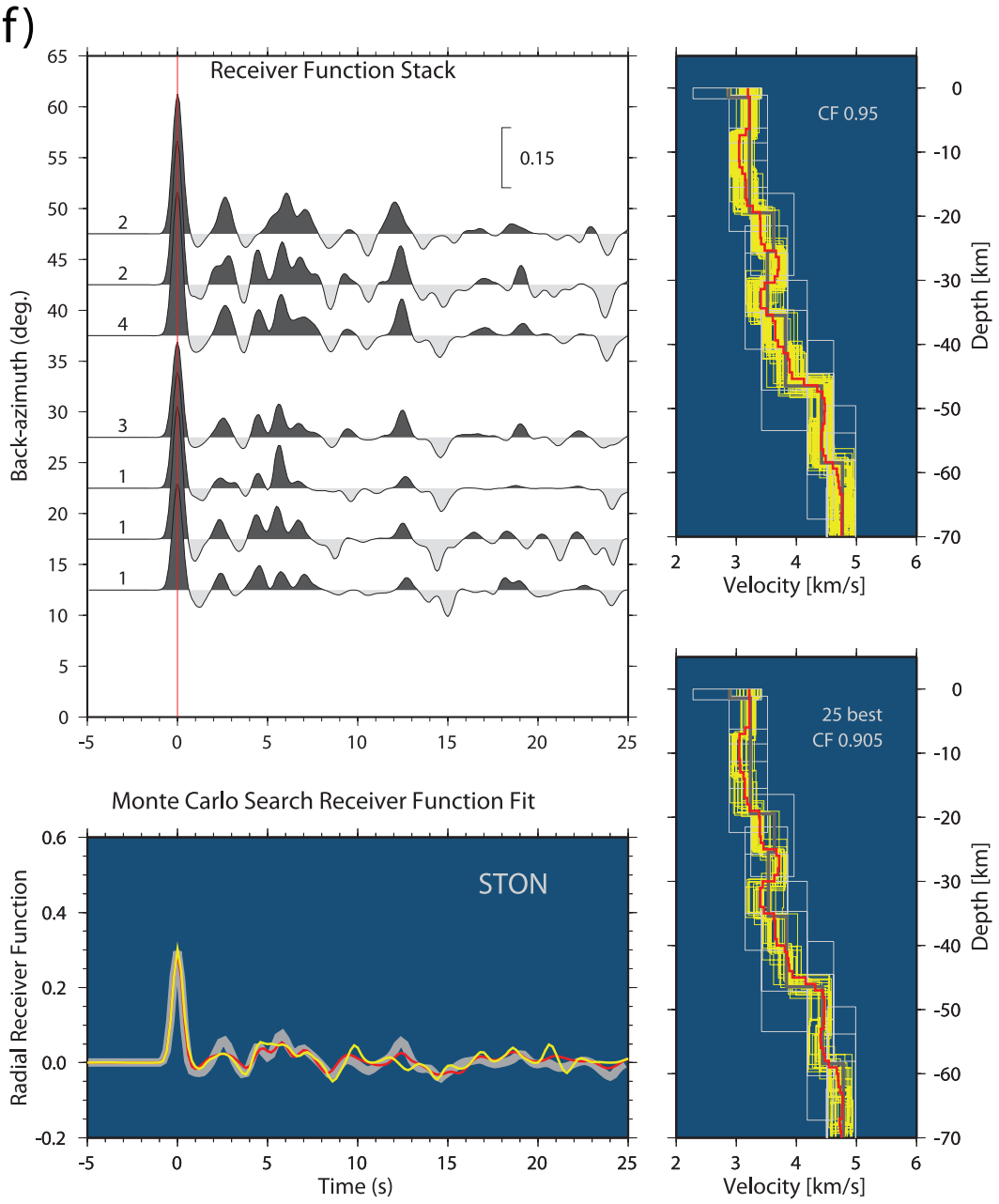

Figure 6. (*Continued.*)

43 ± 2 and 37 ± 0 km, respectively, which approximately agrees with the results from the refraction profiles (Dragašević & Andrić 1968; Skoko *et al.* 1987). The V_p/V_s ratio of 1.92 ± 0.01 is very high. The RFs are similar to those observed at the station RIY. Similarly, the inversion yields upper crust topped by a 4-km-thick layer of relatively small seismic velocity. We found the structure of the upper crust to be fairly complex with several small discontinuities. At the depth of about 30 km a sharp discontinuity divides the upper from the lower crust, which is characterized by a gradual velocity increase until the Moho is reached. The crust–mantle boundary is clear and more pronounced than beneath RIY.

The station KIJV (Fig. 6c) is one of two stations located deeper inland, approximately 50 km from the Adriatic coast. Crustal thickness found from the Monte Carlo inversion and H-κ stacking is 60 ± 2 km and 51 ± 15 km, respectively. This discrepancy is due to the fact that preferred H-κ solution indicates very high V_p/V_s ratio, which is larger than was allowed in the inversion. The secondary maximum in the H-κ plot corresponds well with the range of values obtained the Monte Carlo search. Furthermore, the amplitudes of the main Moho phases (P_s, P_pP_s, $P_pS_s + P_sP_s$) are small, which influences the results of the inversion and the H-κ method. The upper crust is characterized by a drop in shear wave velocity at about 2 km depth, and a gradual increase until a transition to the lower crust is reached at about 28 km. A thin low-velocity layer at shallow depths, although clearly indicated in the inversions, might be just an artefact created by the inversion scheme to accommodate for the small amplitudes in the RFs. Lower crust is characterized by a fairly constant velocity profile, with a hint of decrease just above the mantle.

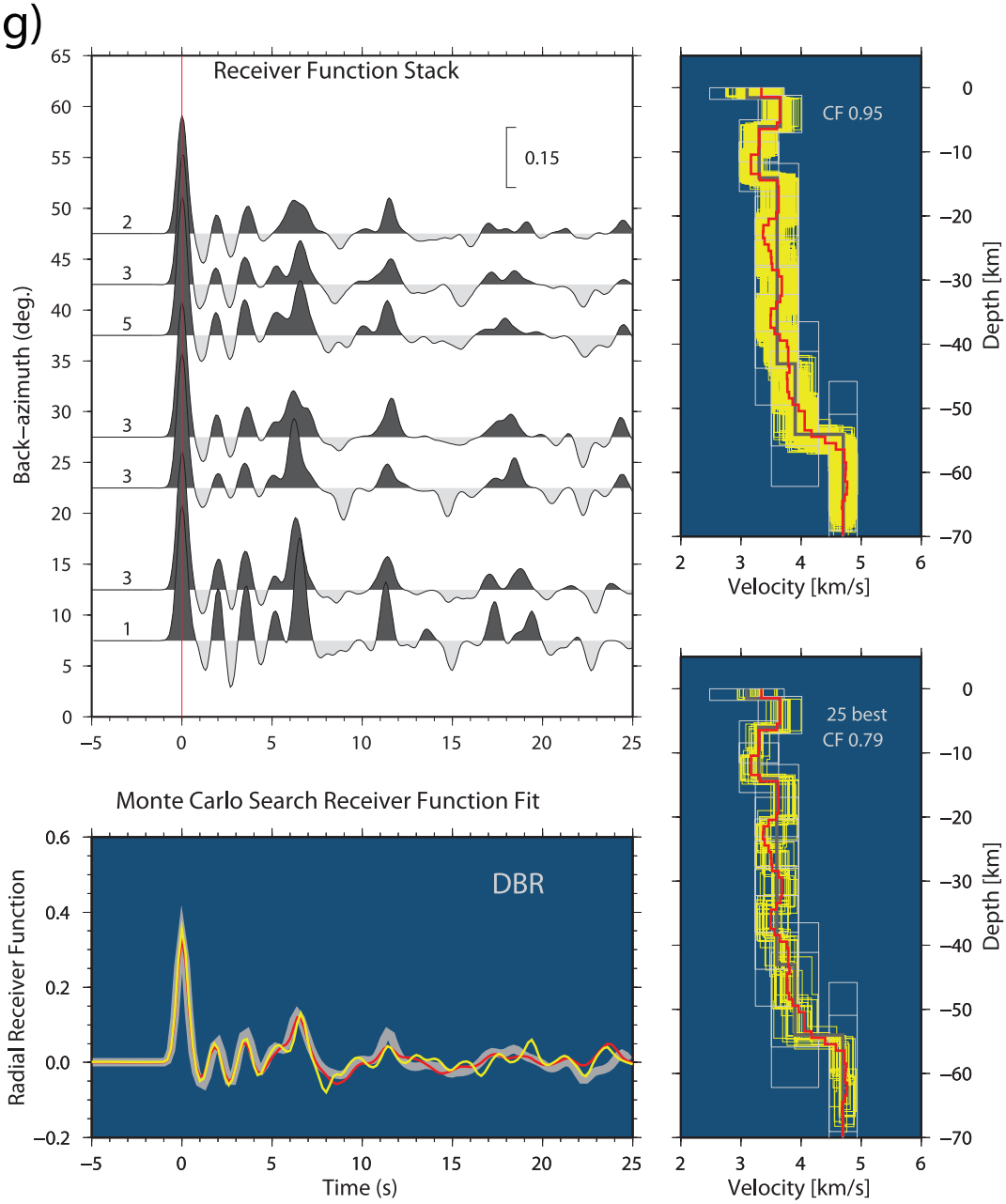

Figure 6. (*Continued.*)

The station CACV (Fig. 6d) is situated to the southeast of KIJV. Crustal structure beneath CACV is characterized by two well-pronounced intracrustal discontinuities. The upper one is located at about 8 km depth and probably marks the boundary between shallower carbonate sediments and a crystalline basement. A deeper discontinuity at 27 ± 2 km depth separates the upper from the lower crust. Results from H-κ and inversions estimate Moho depth at 58 ± 8 km and 56 ± 2 km, respectively. This is significantly deeper than about 42 km thickness found in the DSS experiments of Dragašević & Andrić (1968), and the later map of the Moho topography by Skoko *et al.* (1987). Comparing the results of inversion for the nearby stations KIJV and CACV we see that the final models at both stations point to a very deep Moho with a well-defined intracrustal discontinuity around 27 km. The V_p/V_s ratio for the largest maximum in H-κ stacking has the value of 1.72 ± 0.09.

HVAR (Fig. 6e) is the second island station in this study, located in the Central Adriatic archipelago. Inversions indicate a two-layered crust topped by a thin layer of very low shear wave velocities. The thickness of the upper crust is estimated at 18 km with a clear distinction between the two layers. Its lower part, beginning at 10-km depth, is characterized by the velocity decrease. The depths found for the Moho below HVAR from the inversion and H-κ method are 38 and 46 km, respectively. The estimated value of κ is 1.92 ± 0.12. Similarly to the stations KIJV and CACV, results of the H-κ analyses for this station are somewhat ambiguous because of the obvious trade-off between the crustal thickness and the V_p/V_s (see Fig. 5). The second largest maximum indicates the crustal thickness of 46 ± 8 km and V_p/V_s value of 1.76 ± 0.12, which is within the uncertainties of the Monte Carlo search results. These results are also similar to those of the RF study of van der Meijde *et al.* (2003)

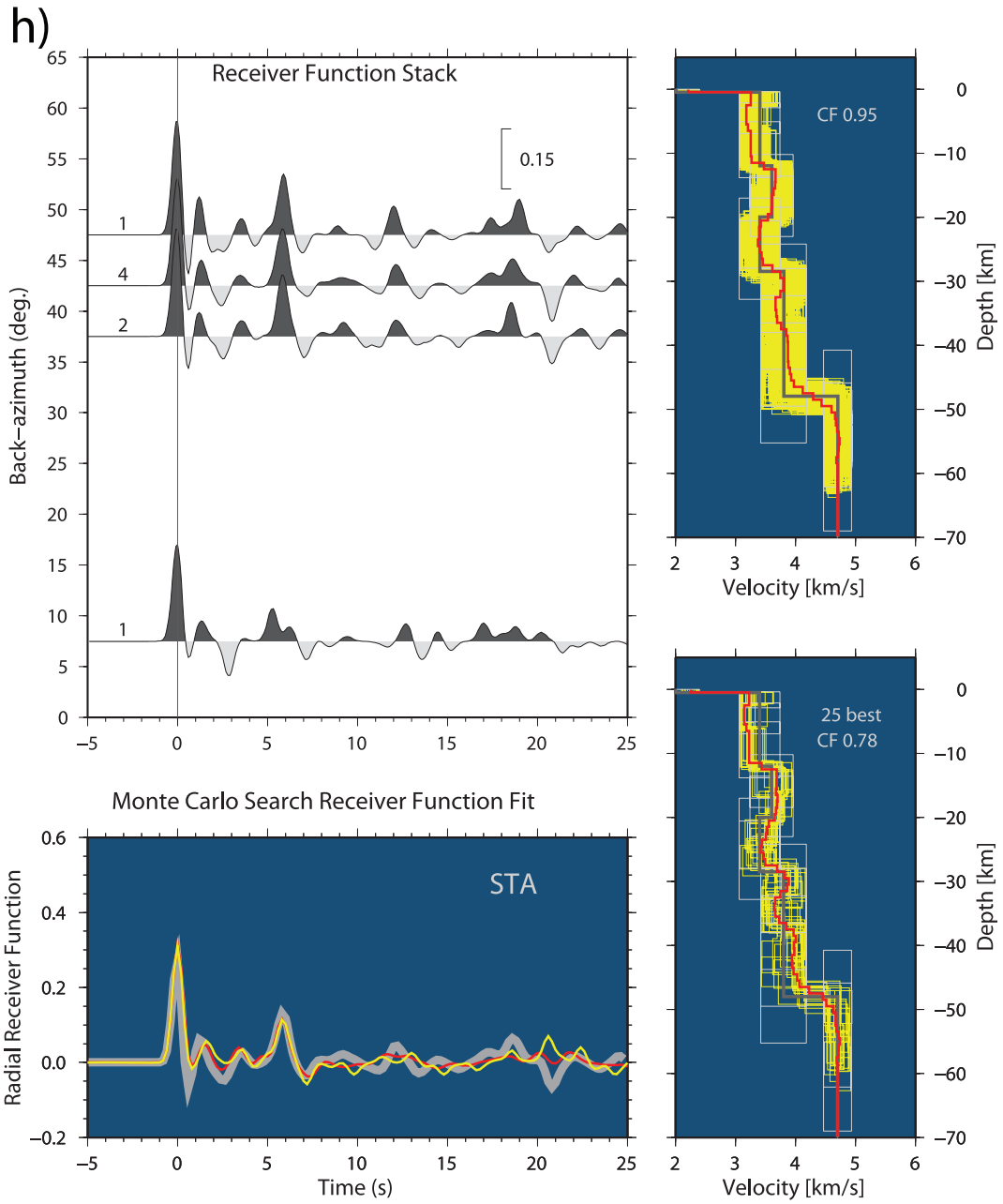

Figure 6. (*Continued.*)

for the same station (with a different, smaller data set). They found 47-km-thick crust with 11 km sedimentary layer at the top, with a smaller V_p/V_s ratio of 1.70. We observe little variation of velocities in the lower crust and a strong velocity contrast at the Moho.

The first of the three southern Adriatic stations is STON (Fig. 6f), which is characterized by the crustal structure without explicit separation into the upper and the lower crust. Of the two discontinuities at the depths of 47 and 60 km, our preferred Moho location is at the more pronounced discontinuity at 47 ± 2 km. H-κ technique yields H = 40 ± 6 km, κ = 1.89 ± 0.16. In the upper part of the crust, shear wave velocity gradually increases until the depth of about 30 km, where we observe a thin low-velocity layer. After that point shear wave velocity increases at a more rapid rate until Moho is reached. Crust-to-mantle transition is characterized by a smaller velocity contrast compared to other stations in this study.

Station DBR (Fig. 6g) is situated between the stations STON and STA in the southern part of the Adriatic coast. RFs, they are rather noisy, and have high amplitude reverberations in the crust, which contributed to large uncertainties and discrepancies of the inferred Moho depths by the two methods used. H-κ yields crustal thickness of 44 ± 2 km with a very high V_p/V_s of 1.90 ± 0.03, whereas inversions give H = 55 ± 2 km. From our modelling, the upper crust is characterized by the high shear wave velocity layer 2 km below the surface and a sudden drop of speeds at about 6 km depth. Below the 8-km-thick layer of relatively low shear wave velocity, seismic velocities remain almost constant in the lower part of the crust.

The southernmost station STA (Fig. 6h) recorded only eight events that produced RFs coherent enough to be stacked and averaged, which is due to the fact that the station operated for only

18 months with various power- and instrument-related problems. Our averaged model is characterized by a very thin layer of low shear wave velocity at the surface and an indication of two intracrustal discontinuities. The first of them lies at the depth of about 11 km and marks the bottom of the carbonate sedimentary rocks. The second discontinuity is located at the depth of 28 km and divides the upper from the lower crust. Estimates of the crustal thickness from H-κ search and inversion give 43 ± 2 and 48 ± 3 km, with the V_p/V_s ratio of 1.89 ± 0.04.

5 DISCUSSION AND CONCLUSIONS

The average crustal thickness beneath the Northern Adriatic stations (RIY and NVLJ) obtained by our multistep RFs modelling methods (the averages of the two approaches are shown in Table 1), are consistent with published results of recent DSS experiments for the Alp07 profile (Šumanovac *et al.* 2009). At the two stations located in the central Dinarides (KIJV and CACV) we observe Mohorovičić discontinuity at depths of 50–55 km, significantly deeper than previous estimates of around 45 km of Skoko *et al.* (1987), which was also adopted in the map of Grad *et al.* (2009). Similar results at the stations KIJV and CACV with well-defined mid-crustal discontinuity around the depth of 29 km and a deep Moho suggest possible overlapping of two tectonic units as the result of the Adria–Dinarides collision, and Adria's counter-clockwise rotation (see Introduction). Currently, there is little independent geophysical evidence supporting such conclusion, which nevertheless fits into some of the new geological and tectonic models of the region. For instance, the profile crossing the Dinarides WSW–ENE in Schmid *et al.* (2008) suggests that the Adriatic microplate is today indeed underthrust below the External Dinaridic platform. In a recent study, Šumanovac (2010b) used all available geophysical and geodetic data to also suggest a geological model where Adriatic structures are underthrust beneath the Dinarides and the Pannonian mantle at a small angle. Crustal thickness of 46 km beneath the mid-Adriatic station HVAR is consistent with the RFs study of van der Meijde *et al*. (2003), but somewhat deeper than 35–42 km determined in the old refraction profiles of Dragašević & Andrić (1968). The results for the three stations located in southern Croatia (STON, DBR and STA) suggest average crustal thickness of 46 km, with the largest deviation being the inversion result at DBR (Table 1), where the RF waveforms are characterized by high-amplitude intracrustal reverberations, which prevented consistent modelling and probably contributed to a high value for the Moho depth. Our crustal thickness is also higher than 35–40 km reported by Dragašević & Andrić (1968).

Discrepancy of the preferred models obtained by the H-κ technique on one side, and the Monte Carlo inversion on the other, would mostly disappear had we constrained the κ-domain to the same V_p/V_s interval as was done in the modelling. Leaving it free resulted in many cases in a very high V_p/V_s exceeding 1.85 which is characteristic of limestone's and dolomites (Christensen 1996; Christensen & Stanley 2003) (which indeed predominate in the sedimentary layers of the uppermost crust) and mostly mafic rocks presumed to prevail in the lower crust. However, the rest of the crust is thought to be composed mostly of clastic and felsic rocks, whose V_p/V_s ratio is lower or close to the one of a Poissonian solid. We therefore expect average value of κ to be below 1.8, which is also consistent with the empirical 1-D model and yielding traveltime curves of the main crustal phases used to locate earthquakes in this area (B.C.I.S. 1972).

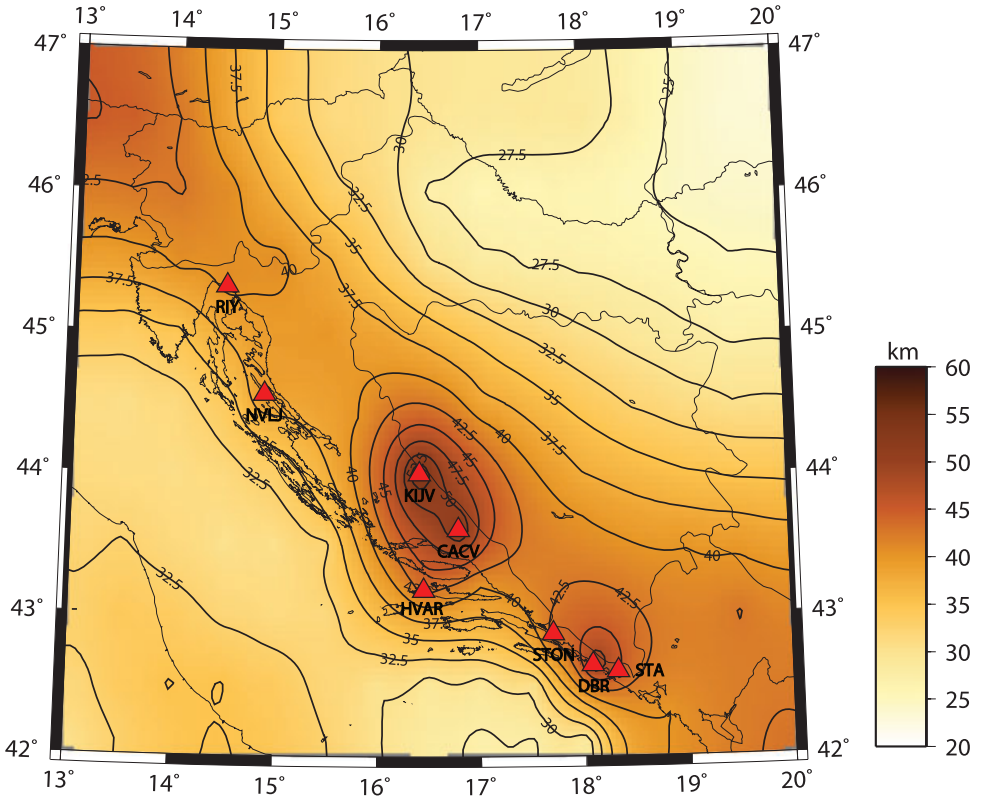

Figure 7. Moho isobaths with point measurements from this study incorporated into selected measurements from Grad *et al.* (2009). Locations of the eight stations from this study are shown by red triangles. Moho depths beneath stations are the average of H-κ and waveform inversion measurements (see Table 1).

We noted no clear systematic variation of the arrival times of any of the various crustal phases with azimuth, at any of the stations (top-left subplots in Figs 6a–h). However, in some cases a systematic variation of RF amplitudes with the backazimuth is observed (e.g. KIJV at 2.5, 7.5 and 11 s; HVAR at 1.3 and 2 s, with a possible duplication of the later phase; STON at 2.5 and 12 s, etc.). This indicates that anisotropy and/or the Moho topography may play a non-negligible role, which remains to be confirmed in subsequent studies.

In Fig. 7 we show our measurements incorporated into selected results from Grad *et al.* (2009) to produce a map of Moho topography beneath Croatia and the neighbouring regions. In general, all the obtained results agree well with an anticipated scheme of the thickest crust under the Dinardies and a bilateral thinning towards the Pannonian Basin on one side and the Adriatic Sea on another. The only somewhat surprising result is a deep crustal root found at the Central Dinarides stations KIJV and CACV. If this can be confirmed by an independent study, it would represent some of the thickest crustal roots in Europe. Future studies of the region will include, *inter alia*, surface wave dispersion measurements to invert jointly with RFs and thus provide better estimates of overall absolute velocity. The 1-D profiles derived in this study will also be used for the calibration of structural Green's functions to allow a complete-waveform moment tensor inversion for significant earthquakes occurring along the Adriatic coast. This should shed more light on the stress regime and help understand complex tectonics of this region.

ACKNOWLEDGMENTS

We thank two anonymous reviewers for their constructive criticism that helped us to improve the overall quality of the manuscript. The study was supported by the Ministry of Science, Education and Sports of the Republic of Croatia through projects 119-1193086-1315 and 119-1193086-1314, the National Foundation for Science, Higher Education and Technological Development of the Republic of Croatia, and the Research School of Earth Sciences of the Australian National University. All support is gratefully acknowledged.

REFERENCES

Aljinović, B., 1977. A review of the seismic exploration carried out in the Dinarides. *Nafta,* **5,** 270–274 (in Croatian).

Aljinović, B., 1983. The deepest seismic horizons in the northeastern Adriatic, *PhD thesis,* University of Zagreb (in Croatian).

Aljinović, B., Blašković, I., Cvijanović, D., Prelogović, E. & Skoko, D., 1984. Correlation of geophysical, geological and seismological data in the coastal part of Yugoslavia, *Boll. Ocean. Teor. Appl.,* **2,** 77–90.

Ammon, C.J., 1991. The isolation of receiver effects from teleseismic *P* waveforms, *Bull. seism. Soc. Am.,* **81,** 2504–2510.

Anderson, H. & Jackson, J., 1987. Active tectonics of the Adriatic region, *Geophys. J. Int.* **91**(3), 937–983, doi: 10.1111/j.1365-246X.1987.tb01675.x.

B.C.S.I., 1972. Tables des tempts de propagation des ondes séismiques, Hodochrones pour la region des Balkans, *Manuel d'utilisation,* Bureau Central International de Séismologie, Strasbourg.

Bennett, R.A. *et al*., 2008. Eocene to present subduction of southern Adria mantle lithosphere beneath the Dinarides, *Geology,* **36**(1), 3–6, doi:10.1130/G24136A.1.

Bianco, F., Del Pezzo, E., Castellano, M., Ibanez J. & Di Luccio, F., 2002. Separation of intrinsic and scattering seismic attenuation in the Southern Apennine zone, Italy, *Geophys. J. Int.,* **150,** 10–22.

Birch, F. 1961. The velocity of compressional waves in rocks to 10 kilobars, part 2, *J. geophys. Res.,* **66,** 2199–2224.

Brückl, E. *et al*., 2007. Crustal structure due to collisional and escape tectonics in the Eastern Alps region based on profiles Alp01 and Alp02 from the ALP 2002 seismic experiment, *J. geophys. Res.,* **112,** B06308, doi:10.1029/2006JB004687.

Brückl, E., Behm, M., Decker, K., Grad, M., Guterch, A., Keller, G.R. & Thybo, H., 2010. Crustal structure and active tectonics in the Eastern Alps, *Tectonics,* **29,** TC2011, doi:10.1029/2009TC002491.

Cassidy, J.F., 1992. Numerical experiments in broadband receiver function analysis, *Bull. seism. Soc. Am.,* **82,** 1453–1474.

Calais, E., Nocquet, J.-M., Jouanne, F. & Tardy, M., 2002. Current extension in the Central Part of the Western Alps from continuous GPS measurements, 1996–2001, *Geology,* **30–37,** 651–654.

Chen, Y., Niu, Liu, R., Huang, Z., Tkalčić, H., Sun, L. & Chan, W., 2010. Crustal structure beneath China from receiver function analysis, *J. geophys. Res*., **115,** B03307, doi:10/1029/2009JB006386.

Chevrot, S. & Van Der Hilst, R. D., 2000. The Poisson ratio of the Australian crust: geological and geophysical implications, *Earth planet. Sci. Lett.,* **183,** 121–132.

Christensen, N.I. & Mooney, W.D., 1995. Seismic velocity structure and composition of the continental crust: a global view, *J. geophys. Res*., **110,** B7, 9761–9788.

Christensen, N.I., 1996. Poisson's ratio and crustal seismology, *J. geophys. Res*., **101,** B2, 3139–3156.

Christensen, N.I. & Stanley, D., 2003. Seismic velocities and densities of rocks, in *International Handbook of Earthquake and Engineering Seismology,* pp. 1587–1594, eds Lee, H.K., Kanamori, H. & Jennings, P.C., Academic Press, London.

Di Bona, M., Lucente, F.P. & Piana Agostinetti, N., 2008. Crustal structure and Moho depth profile crossing the central Apennines (Italy) along the N42° parallel, *J. geophys. Res.,* **113,** B12306, doi:10.1029/2008JB005625.

Doglioni, C. & Carminati, E., 2002. The effects of four subductions in NE-Italy, *Mem. Sci. Geol.,* **54,** 1–4.

Dragašević, T. & Andrić, B., 1968. Deep seismic soundings of the Earth's crust in the area of the Dinarides and the Adriatic sea, *Geophys. Prospect.,* **16,** 54–76.

Efron, B. & Tibshirani, R., 1986. Bootstrap methods for standard errors, confidence intervals, and other measures of statistical accuracy, *Stat. Sci.,* **1,** 54–75.

Faccenna, C., Piromallo, C., Crespo-Blanc, A., Jolivet, L. & Rossetti, F., 2004. Lateral slab deformation and the origin of the western Mediterranean arcs, *Tectonics,* **23,** 1012–1036.

Geissler, W.H., Kind, R. & Yuan X.Y., 2008. Upper mantle and lithospheric heterogeneities in central and eastern Europe as observed by teleseismic receiver functions, *Geophys. J. Int.,* **174,** 351–376.

Grad, M., Tiira, T. & ESC Working Group, 2009. The Moho depth map of the European Plate, *Geophys. J. Int.,* **176,** 279–292.

Herak, D. & Herak, M., 1995. Body-wave velocities in the circum-Adriatic region, *Tectonophysics,* **241,** 121–141.

Herak, M., 1990. Velocities of the body waves in the Adriatic region, *Boll. Geofis. Teor. Appl.,* **XXXII**(125), 11–18.

Herak, D., Herak, M., Prelogović, E., Markušić, S. & Markulin, Ž., 2005. Jabuka island (Central Adriatic Sea) earthquakes of 2003, *Tectonophysics,* **398,** 167–180.

Ivančić, I., Herak, D., Markušić, S., Sović, I. & Herak, M., 2006. Seismicity of Croatia in the period 2002–2005, *Geofizika,* **23**(2), 87–103.

Julia, J., Ammon, C.J. & Herrmann, R.B., 2003. Lithospheric structure of the Arabian Shield from the joint inversion of receiver functions and the surface wave dispersion, *Tectonophyiscs,* **371,** 1–21.

Langston, C.A., 1979. Structure under Mount Rainier, Washington, inferred from teleseismic body waves, *J. geophys. Res.,* **84,** 4749–4762.

Ligorría, J.P. & Ammon, C.J., 1999. Iterative deconvolution and receiver function estimation, *Bull. seism. Soc. Am.,* **89,** 1395–1400.

Lippitsch, R., Kissling, E. & Ansorge, J., 2003. Upper mantle structure beneath the Alpine orogen from high-resolution teleseismic tomography, *J. geophys. Res.,* **108** (B8), 2376, doi:10.1029/2002JB002016.

Márton, E. 2006. Paleomagnetic evidence for Tertiary counterclockwise rotation of Adria with respect to Africa, in *The Adria Microplate: GPS*

Geodesy, Tectonics and Hazards, pp. 71–80, eds Pinter, N., Grenerczy, G., Weber, J., Stein, S. & Medak, D, NATO Science Series, Springer.

Mayeda, K., Koyanagi, S., Hoshiba, M., Aki, K. & Zeng, Y., 1992. A comparative study of scattering, intrinsic, and coda Q-1 for Hawaii, Long Valley, and central California between 1.5 and 15.0 Hz, *J. geophys. Res.,* **97,** 6643–6659.

Mele, G. & Sandvol, E., 2003. Deep crustal roots beneath the Northern Apennines inferred from teleseismic receiver functions, *Earth planet. Sci. Lett.,* **211,** 69–78.

Mohorovičić, A., 1910. Potres od 8.X 1909 (Das Beben vom 8.X. 1909), Jahrbuch des meteorologischen Observatoriums in Zagreb (Agram) für das Jahr 1909, 1–56 (English translation: 1992, Earthquake of 8 October 1909, *Geofizika,* **9,** 3–55).

Niu, F. & James, D.E., 2002. Fine structure of the lowermost crust beneath the Kaapvaal craton and its implications for crustal formation and evolution, *Earth planet. Sci. Lett.,* **200,** 121–130.

Nocquet, J.M., & Calais, E., 2004. Geodetic measurements of crustal deformation in the western Mediterranean and Europe, *Pure appl. Geophys.,* **161,** 661–681.

Oldow, J.S. *et al*., 2002. Active fragmentation of Adria, the north African promontory, central Mediterranean orogen, *Geology,* **30**(9), 779–782.

Owens, T.J., Taylor, S.R. & Zandt, G., 1987. Crustal structure at regional seismic test network stations determined from inversion of broad-band teleseismic *P* waveforms, *Bull. seism. Soc. Am.,* **77,** 631–632.

Park, J. & Levin, V., 2000 Receiver functions from multiple-taper spectral correlation estimates, *Bull. seism. Soc. Am.,* **90**(6), 1507–1520, doi:10.1785/0119990122.

Piana-Agostinetti, N., Lucente, F.P., Selvaggi, G. & Di Bona, M., 2002. Crustal structure and the Moho beneath Northern Appenines (Italy), *Geophy. Res. Lett.,* **29**(20), 1999, doi:10.1029/2002GL015109.

Piana-Agostinetti, N. & Amato, A., 2009. Moho depth and V_p/V_s ratio in peninsular Italy from teleseismic receiver functions, *J. geophys. Res.,* **114,** B06303, doi:10.1029/2008JB005899.

Piromallo, C. & Morelli, A., 2003. *P* wave tomography of the mantle under the Alpine-Mediterranean area, *J. geophys. Res.,* **108,** 2065, doi:10.1029/2002JB001757.

Saftić, B., 2003. *Naftno-geološki Potencijal Jugozapadnog Ruba Panonskog Bazena (Petroleum-Geological Potential of the Southwestern Margin of the Pannonian Basin),* Expert Document Fund, INA-Oil Industry, Zagreb.

Sandvol, E., Seber, D., Barazangi, M., Vernon, F.R., Mellors, R. & Al-Amri, A.M., 1998. Lithospheric seismic velocity discontinuities beneath the Arabian Shield, *Geophys. Res. Lett.,* **23,** 1829–1832.

Schmid, S.M. *et al*., 2008. The Alpine-Carpathian-Dinaridic orogenic system: correlation and evolution of tectonic units, *Swiss J. Geosci.,* **101,** 139–183. doi:10.1007/s00015–008-1247–3.

Skoko, D., Prelogović, E. & Aljinović, B., 1987. Geological structure of the Earth's crust above the Moho discontinuity in Yugoslavia. *Geophys. J. R. astr. Soc.,* **89,** 379–382.

Šumanovac, F., Orešković, J., Grad, M. & ALP 2002 Working Group, 2009. Crustal structure at the contact of the Dinarides and Pannonian basin based on 2-D seismic and gravity interpretation of the Alp07 profile in the ALP2002 experiment, *Geophys. J. Int.,* **179,** 615–633. doi:10.1111/j.l365–246X.2009.04288.x.

Šumanovac, F., 2010a. Lithosphere structure at the contact of the Adriatic microplate and the Pannonian segment based on the gravity modelling, *Tectonophysics,* **485,** 98–106, doi:10.1016/j.tecto.2009.12.005.

Šumanovac, F., 2010b. Crustal structure and Mohorovičić discontinuity at the contact of the Adriatic microplate and the Pannonian segment. *Abstract Book ESC 2010,* 2010 September 6–10, Montpellier, France.

Tesauro, M., Kaban, M.K. & Cloetingh, S.A.P.L., 2008. EuCRUST-07: a new reference model for European crust, *Geophys. Res. Lett.,* **35,** 5313–5318. doi:10.1029/2007GL032244.

Tkalčić, H., Pasyanos, M.E., Rodgers, A.J., Gök, R., Walter, W.R. & Al-Amri, A., 2006. A multistep approach for joint modelling of surface wave dispersion and teleseismic receiver functions: implications for lithospheric structure of the Arabian Peninsula, *J. geophys. Res.,* **111,** 11 311–11 336.

Tkalčić, H. & Banerjee, D., 2009. Interactive Receiver Functions Forward Modeller (IRFFM). Software and manual available at: http:/www.rses.anu.edu.au/hrvoje/IRFFMv1.1.html (last accessed 2010 December 9).

Tomljenović, B., 2002. Structural assemblage of Medvednica and Samoborsko gorje Mts, *PhD thesis*. University of Zagreb.

Van Der Meijde, M., Van der Lee, S. & Gardini, D., 2003. Crustal structure beneath broad-band seismic stations in the Mediterranean region, *Geophys. J. Int.,* **152,** 729–739.

Zhu, L. & Kanamori, H., 2000. Moho depth variation in southern California from teleseismic receiver functions, *J. geophys. Res.,* **105,** 2969–2980.

Ziegler, P.A. & Dèzes, P., 2006. Crustal evolution of Western and Central Europe, *Mem. Geol. Soc. Lond.,* **32,** 43–56.